American Journal of Botany

American Journal of Botany 98(1): 76–87. 2011.

Old–New World and trans-African disjunctions of *Thamnosma* (Rutaceae): Intercontinental long-distance dispersal and local differentiation in the succulent biome[1]

Mike Thiv[2,7], Timotheüs van der Niet[3], Frank Rutschmann[4], Mats Thulin[5], Thomas Brune[6], and Hans Peter Linder[4]

[2]Botany Department, State Museum of Natural History Stuttgart, Rosenstein 1, 70191 Stuttgart, Germany; [3]School of Biological and Conservation Sciences, University of KwaZulu-Natal, Private Bag X01, Scottsville 3209, South Africa; [4]Institute for Systematic Botany, University of Zurich, Zollikerstrasse 107, 8008 Zurich, Switzerland; [5]Department of Systematic Biology, Uppsala University, Norbyvägen 18D 75236 Uppsala, Sweden; and [6]Institute of Food Science and Biotechnology, University of Hohenheim, Garbenstrasse 25, 70593 Stuttgart, Germany

- *Premise of the study*: The succulent biome is highly fragmented throughout the Old and New World. The resulting disjunctions on global and regional scales have been explained by various hypotheses. To evaluate these, we used *Thamnosma*, which is restricted to the succulent biome and has trans-Atlantic and trans-African disjunctions. Its three main distribution centers are in southern North America, southern and eastern Africa including Socotra.
- *Methods*: We conducted parsimony, maximum likelihood, and Bayesian phylogenetic analyses based on chloroplast and nuclear sequence data. We applied molecular clock calculations using the programs BEAST and MULTIDIVTIME and biogeographic reconstructions using S-DIVA and Lagrange.
- *Key results*: Our data indicate a weakly supported paraphyly of the New World species with respect to a palaeotropical lineage, which is further subdivided into a southern African and a Horn of Africa group. The disjunctions in *Thamnosma* are mostly dated to the Miocene.
- *Conclusions*: We conclude that the Old–New World disjunction of *Thamnosma* is likely the result of long-distance dispersal. The Miocene closure of the arid corridor between southern and eastern Africa may have caused the split within the Old World lineage, thus making a vicariance explanation feasible. The colonization of Socotra is also due to long-distance dispersal. All recent *Thamnosma* species are part of the succulent biome, and the North American species may have been members of the arid Neogene Madro-Tertiary Geoflora. Phylogenetic niche conservatism, rare long-distance dispersal, and local differentiation account for the diversity among species of *Thamnosma*.

Key words: biogeography; disjunctions; Madro-Tertiary flora; molecular dating; phylogeny; Rutaceae; succulent biome; *Thamnosma*.

Schrire et al. (2005b) accounted for the diversification of legumes with a model that incorporated phylogenetic niche conservatism with local differentiation. The tendency of lineages to retain their ancestral ecological niche rather than adapting to new environments (phylogenetic niche conservatism) has has been demonstrated in diverse clades and regions (Wiens, 2004; Donoghue, 2008; Crisp et al., 2009). On the basis of phylogenetic niche conservatism, widely distributed clades should occupy similar habitats in remote areas, a pattern neatly demonstrated in the legumes (Lavin et al., 2004; Schrire et al., 2005b). The succulent biome, which is characterized by a climate with a long dry season, is found in relatively small fragments and isolated regions in both South and North America, in a large region in SW Africa, and from Tanzania to Pakistan. The predominant growth forms in these climates are usually evergreen, sclerophyllous, nonfire-adapted shrubs and succulents (Mooney and Dunn, 1970; Schrire et al., 2005a). This succulent biome has been the object of some studies (e.g., Lavin et al., 2004; Schrire et al., 2005a, b, 2009). Its characteristic climate and highly fragmented distribution make it an excellent system in which to investigate the effects of niche conservatism.

The succulent biome shows a disjunction between the New and the Old World. This pattern is matched by the distribution of legumes where, e.g., the genera *Arcoa* Urb., *Diphysa* Jaqu., *Pictetia* DC., and *Chapmannia* Torr. & Gray occur in North and Mesoamerica and *Tetrapterocarpon* Humbert, *Zygocarpum* Thulin & Lavin, *Ormocarpopsis* R.Vig., *Ormocarpum* P. Beauv., and *Chapmannia* occur in Africa. In most of these cases, the New World group finds its corresponding sister clade in Africa. Several hypotheses were assumed to explain this pattern. Inferring

[1] Manuscript received 6 September 2010; revision accepted 23 November 2010.

The authors would like to thank Jon Rebman (SDSU, USA) and Michael Denslow (Rancho Santa Ana Botanic Garden, USA) for providing plant material, Joachim Kadereit (Mainz, Germany) for helpful comments on the manuscript, and Mohamed Ali Hubaishan (AREA Research Station Mukalla), Ahmed Said Sulaiman (EPA Socotra), Said Masood Awad Al-Gareiri (Dept. Agriculture Socotra), and Mohamed El-Mashjary (EPA Sanaa, all Yemen) for support of the fieldwork in Socotra. The fieldwork was conducted as part of the BIOTA Yemen Project funded by the German Ministry for Research and Education (BMBF). The work was supported by grants of the German Research Foundation (DFG, Th830/1-1) and the Claraz-Schenkung (Switzerland) to M.T.

[7] Author for correspondence (e-mail: mike.thiv@smns-bw.de)

doi:10.3732/ajb.1000339

from physiognomical similarities, links have been proposed between succulent biome taxa and dry boreotropical and Madrean-Tethyan representatives (Lavin et al., 2000). Based on palaeontological and geological evidence, Tiffney (1985b) proposed an Eocene North Atlantic Land bridge (55.8–33.9 million years ago [Ma]) linking the continents of the Northern Hemisphere, resulting in a circumboreal, deciduous, and evergreen heterogenous flora (boreotropical hypothesis, Wolfe, 1975). Lavin et al. (2000) suggested that vicariance between North/Mesoamerica and Africa was possible via this land bridge for legumes. Similarily, only younger in time, the Madrean-Tethyan hypothesis suggested a common occurrence of recent and fossil sclerophyllous taxa in both southwestern North America and the Old World by the late Eocene to the late Paleogene (37.2–23 Ma, Axelrod, 1972, 1973, 1975). Another possible vicariant origin of this disjunction may have been caused by an early Miocene (23–16 Ma) migration route via the Bering land bridge, as suggested by Stebbins and Day (1967) and Tiffney (1985a). In contrast to these vicariance scenarios, the intercontinental disjunction of legumes in the succulent biome was recently interpreted as result of long distance because the ages of these lineages are much younger than the assumed vicariance events (Lavin et al., 2004).

The succulent biome is also disjunct on the African continent. Numerous plants (e.g., *Aizoon* L. [Aizoaceae], *Trichoneura* Anderss. [Poaceae]) and animals (e.g., ostriches) occupy an "arid corridor" between southwestern and northeastern Africa (Balinsky, 1962; Verdcourt, 1969; de Winter, 1971; Jürgens, 1997), with an extension to Mauretania (NW Africa). The closure and widening of this arid track has been linked to Miocene uplift and rifting in Central Africa and climate changes in the Pleistocene (Caujape-Castells et al., 2001; Coleman et al., 2003), which have led to isolated populations in these areas characterized by a short rainy season. Evidence supporting the arid track came from phylogeographical studies of ostriches (Freitag and Robinson, 1993) and phylogenetic investigations of *Androcymbium* Willd. (Colchicaceae, Caujape-Castells et al., 2001), *Senecio* L. (Coleman et al., 2003), and *Zygophyllum* L. (Zygophyllaceae, Bellstedt et al., 2008).

A small transoceanic disjunction in the succulent biome is found in the Horn of Africa region. This area covers the three provinces of the Eritreo–Arabian subregion of Takhtajan (1986): Somalo-Ethiopia, South Arabia, and the Socotran archipelago. Socotra is of continental origin and separated from the Arabian plate about 15–18 Ma (Richardson et al., 1995; Fleitmann et al., 2004; Van Damme, 2009). In all three regions, the succulent biome is prevalent, leading to two explanations for Socotran–continental disjunctions. They are either vicariant relicts preceeding the rifting (postulated for chameleons; Macey et al., 2008), or were established by long-distance dispersal over water (e.g., *Aerva* Forssk. [Amaranthaceae], Thiv et al. [2006]; *Echidnopsis* Hook. f. [Apocynaceae-Asclepiadoideae], Thiv and Meve [2007]; and *Campylanthus* Roth [Plantaginaceae], Thiv et al. [2010]).

To explore the evolution of these disjunctions, we used the rutaceous genus *Thamnosma* Torr. & Frém. With only 11 species, *Thamnosma* occurs in three widely disjunct centers of distribution. Five species grow in southwestern North America, these could well be relicts of the North American Madro-Tertiary geoflora (Axelrod, 1958), an assemblage of sclerophyllous and microphyllous taxa that were adapted to conditions of low annual precipitation, high summer temperatures, and long sunshine periods. The other species are mainly found in Africa, where three species occur in the southern continent from Angola to the northern regions of South Africa, and another three species grow around the Horn of Africa extending to southern Arabia and the island of Socotra (Thulin, 1999) (Table 1, Fig. 1). This pattern with trans-Atlantic and trans-African disjunctions of the succulent biome makes *Thamnosma* a suitable case study (1) to test the hypotheses on the origin of Old and New World disjunctions in the succulent biome, (2) to investigate the "arid corridor" between southern Africa and the Horn of Africa region, and (3) to evaluate a vicariance origin for the Socotran taxon.

MATERIALS AND METHODS

Taxon sampling—To resolve the interspecific phylogenetic relationships of *Thamnosma*, we included all 11 species of *Thamnosma* (Johnston, 1983; Thulin, 1999) in a combined analysis of the ITS, *matK*, and the *atpB-rbcL* spacer (Table 2), rooted with the the closely related *Ruta* L. (Salvo et al., 2008). On the basis of three chloroplast markers, *Thamnosma* is closely related to the eastern Asian, monotypic *Boenninghausenia* Reichb. ex Meissner, *Ruta* L., *Haplophyllum* A. Juss., and *Cneoridium dumosum* Hook. f. (Salvo et al., 2008). Of those, only *Cneoridium* Hook. f. and *Ruta* could be included in our study due to availability of material. Salvo et al. (2008) found a sister-group relationship between *Thamnosma* and *Boenninghausenia*. Still, the monotypic *Psilopeganum* Hemsl. ex Forb. & Hemsl., restricted to a small area of central China (Song et al., 2004), may also be closely related to *Thamnosma*, because these are the only bicarpellate genera in the Rutinae and share capitate stigmas and similar flower merosity and seed shapes (Engler, 1897, 1931; Salvo et al., 2008). This relationship is also supported by phytochemical data (acridones of type H1; da Silva et al., 1988). Because *Psilopeganum* shares more morphological synapomorphies with *Thamnosma* rather than with *Boenninghausenia* (cf. Salvo et al., 2008), it seems more likely that *Thamnosma* and *Psilopeganum* are phylogenetic sisters. However, it is unlikely that *Psilopeganum* is embedded in *Thamnosma* because they differ in the degree of carpel fusion and the size of their disc (Engler, 1897, 1931). No DNA is available for *Psilopeganum*; thus these morphologically based interpretations have not yet been tested. Material was mostly taken from herbarium specimens or, in some cases, silica-gel-dried leaves. Vouchers and EMBL accession numbers are given Table 2.

To estimate the ages of biogeographically relevant nodes in the *Thamnosma* phylogeny, we assembled a set of species representing all major clades of Rutaceae and two taxa with reliable fossils for the *rbcL* analysis. *Thamnosma* was

TABLE 1. Species of *Thamnosma*, their distribution and defined areas of endemism: H = Horn of Africa region, *N* = Northern/ Mesoamerica, S = Southern Africa.

Taxon	Species distribution	Area of endemism
Thamnosma africana Engl.	S Angola, Namibia	S
Thamnosma crenata (Engl.) Thulin	South Africa, Northern Province	S
Thamnosma hirschii Stapf	Yemen, Oman, N Somalia, Socotra	H
Thamnosma montana Torr. & Frém.	S USA, Mexico	N
Thamnosma pailensis M. C. Johnst.	Mexico, SE Coahuila	N
Thamnosma rhodesica (Bak. f.) Mendonça	S+W Zimbabwe, Botswana	S
Thamnosma socotrana Balf. f.	Yemen, Socotra	H
Thamnosma somalensis Thulin	NE Somalia	H
Thamnosma stanfordii I. M. Johnst.	Mexico, S Coahuila	N
Thamnosma texana Torr.	S USA, Mexico	N
Thamnosma trifoliata I. M. Johnst.	Mexico, Baja California	N

Fig. 1. Distribution map (http://www.aquarius.ifm-geomar.de) of *Thamnosma* in North and Central America and in Africa.

represented by six North American and Old World species: southern African *Thamnosma* species were not included because amplifications did not succeed, possibly from degradation of the DNA extracted from herbarium material. Due to the use of degraded DNA from herbarium material, phylogenetic reconstruction and molecular dating were based on only half of the gene length of *rbcL* (790–813 bp).

Laboratory work—The molecular work followed standard protocols. For DNA extraction, the DNeasy plant extraction kit (Qiagen) was used according to the manufacturer's protocol. Amplifications were performed using 1.5 mM buffer, 0.625 mM $MgCl_2$, 0.2 mM dNTPs, 0.05 U/μL *Taq* DNA polymerase (Amersham Biosciences, Freiburg, Germany), 0.325 μM primer, and 5 ng/μL DNA template. PCR profiles included 33 cycles of 94°C for 1 min, 50–55°C for 1 min, and 72°C for 2–3 min. For amplifications and sequencing, the following primers were used. ITS nrDNA: ITS-A 5′-GGAAGGAGAAGTCGTAACAAGG-3′, ITS-B 5′-CTTTTCCTCCGCTTATTGATATG-3′, ITS-D 5′-CTCTCGGCAACGGATATCTCG-3′ (all Blattner, 1999), ITS-R2 5′-CGTTCAAAGACTCGATGGTTC-3′ (von Balthazar et al., 2000). Multiple DNA extractions and ITS sequencing for several accessions of *Thamnosma*, yielded identical results indicating the absence of paralogous copies of ITS. The *atpB-rbcL* intergenic spacer: atpB-F2 5′-GAAGTAGTAGGATTGATTCTC-3′, atpB-R5 5′-GAAGTAGTAGGATTGATTCTC-3′ (both Manen et al., 1994); *matK* (these primers amplify the 3′ end of the *matK* gene and the adjacent intron): matK-Th-F 5′-TTATTCATCTGATTGGATCAT-3′ (designed in the present study), matK-1R 5′-GAACTAGTCGGATGGAGTAG-3′ (Sang et al., 1997); *rbcL*: rbcL-F1 5′-TCACCACAAACAGARACTAAAGC-3′, rbcL-R2 5′-RCGRTGRATGTGAAGAAG-3′ (both Long-Yin Qiu, University of Michigan, personal communication). The use of herbarium material only allowed the amplification of a partition of *rbcL*. PCR products were cleaned using the PCR purification kit (Qiagen, Hilden, Germany). Cycle sequencing was conducted using ABI PRISM BigDye 2.1 to obtain double stranded sequences. Resulting products were analyzed using automated sequencing systems ABI PRISM 3100 (PE Biosystems, Darmstadt, Germany).

Phylogenetic analysis—Sequences of all *Thamnosma* species were aligned using the program Clustal X version 1.81 (Thompson et al., 1997) and then manually adjusted. The alignments are available in TreeBase (S10787, http://treebase.org). First, parsimony (MP) bootstrap analyses (options given later) were conducted for both chloroplast and nuclear data. To test for congruence between these two data sets, we conducted a partition homogeneity test as implemented in the program PAUP* 4.0b10 (Swofford, 1998). Because this test failed to reject the hypothesis of congruency, the two data sets were combined (Johnson and Soltis, 1998; Wiens, 1998). Maximum likelihood (ML; Felsenstein, 1981) and parsimony analyses for the combined data were performed using PAUP* 4.0b10. For the ML analysis, the GTR+I+Γ model was used as indicated by the Akaike information criterion (AIC) in the program Modeltest 3.06 (Posada and Crandall, 1998). For parsimony analyses, characters were equally weighted, character states were treated as unordered, and indels were treated as missing data. Parsimony analyses were carried out using 10^3 random-addition-sequence replicates, with Multrees in effect and tree-bisection-reconnection (TBR) swapping. Parsimony bootstrap analyses (10^4 replicates) were calculated using the closest Multrees and TBR options. Additionally, Bayesian inference using the combined data set was explored using the program MrBayes v. 3.1.2 (Huelsenbeck and Ronquist, 2001). The GTR+Γ model was selected by AIC in the program MrModeltest (Nylander, 2004). Two runs using four parallel chains of 5×10^6 generations with heats of 1.00, 0.83, 0.71, and 0.62 were performed, with a sample frequency of 10^2. Trees from the first 10^4 generations were discarded.

We tested alternative scenarios using a parametric bootstrap analysis. This test is shown to be a statistically sound method of evaluating different alternative topological hypotheses (Huelsenbeck et al., 1996; Goldman et al., 2000; Stefanović and Olmstead, 2004). This procedure included the determination

TABLE 2. Taxon sampling, vouchers and new EMBL numbers for this study. Herbaria acronyms are according to Index Herbariorum (http://sciweb.nybg.org/science2/IndexHerbariorum.asp).

Taxon	Collector	No.	Origin	voucher	ITS1	ITS2	*matK*	*atpB-rbcL* spacer	*rbcL*
Cneoridium dumosum Hook.f.	Thibault et Denslow	s.n.	Cult. Rancho Santa Ana Botanic Garden RSA674337	RSA					FN552678
Euodia hupehensis Dode	Wagen	s.n.	Cult. Bot. Garden Zurich	Z					FN552679
Ruta chalepensis L.	Wagen	s.n.	Cult. Bot. Garden Zurich	Z	FN552647	FN552663	FN552615	FN552631	
Thamnosma africana	Goldblatt et al.	8927	Namibia	MO	FN552649	FN552665	FN552617	FN552633	
Thamnosma africana	Lavranos	21900	Namibia	MO	FN552648	FN552664	FN552616	FN552632	
Thamnosma crenata	Venter	11224	South Africa	MO	FN552650	FN552666	FN552618	FN552634	
Thamnosma hirschii	Miller	10000	Yemen, Socotra	B	FN552651	FN552667	FN552619	FN552635	
Thamnosma hirschii	Kilian & Hein	NK 6164	Yemen	B	FN552653	FN552669	FN552621	FN552637	
Thamnosma hirschii	Thiv	3187	Yemen, Socotra	Z	FN552652	FN552668	FN552620	FN552636	FN552680
Thamnosma montana	Landrum et Landrum	9022	USA, Arizona	NY	FN552654	FN552670	FN552622	FN552638	FN552681
Thamnosma montana	White	4252	USA, California	BM	FN552655	—	FN552623	FN552639	FN552682
Thamnosma pailensis	Woodruff	369	Mexico, Coahuila	BM	FN552656	FN552671	FN552624	FN552640	FN552683
Thamnosma rhodesica	Blomberg et al.	BMP 104	Botswana	UPS	FN552657	FN552672	FN552625	FN552641	
Thamnosma socotrana	Thiv	3176	Yemen, Socotra	STU, Z	FN552658	FN552673	FN552626	FN552642	
Thamnosma socotrana	Kilian	2495	Yemen, Socotra	B					FN552684
Thamnosma somalensis	Thulin et al.	9489	Somalia	UPS	FN552659	FN552674	FN552627	FN552643	
Thamnosma stanfordii	Chiang et al.	9545	Mexico, Coahuila	MO, NY	FN552660	FN552675	FN552628	FN552644	
Thamnosma texana	McGolderick	s.n.	USA, Texas	L	FN552661	FN552676	FN552629	FN552645	FN552685
Thamnosma trifoliata	Rebman	7577	Mexico, Baja California	SD	FN552662	FN552677	FN552630	FN552646	FN552686

of ML parameters for the described constrained topologies. Based on these parameters, 99 simulated data sets were created using the program Seq-Gen (Rambaut and Grassly, 1997). The simulated data sets were analyzed using maximum parsimony with the closest sequence addition and TBR branch swapping, testing for significant differences in lengths between the constrained tree as null hypothesis and the optimal tree.

Molecular dating—We used a molecular clock to date the disjunction between New and Old World species of *Thamnosma*. Based on a likelihood ratio (LR) test (Felsenstein, 1981; Sanderson, 1998; Nei and Kumar, 2000), substitution rates of the *rbcL* sequences were near clock-like. Nonetheless, we employed Bayesian dating using a relaxed clock. This method (Thorne et al., 1998; Thorne and Kishino, 2002) uses a probabilistic model to describe the change in evolutionary rate over time and uses the Markov chain Monte Carlo (MCMC) procedure to derive the posterior distribution of rates and time. It allows multiple calibration points and provides direct credibility intervals for estimated divergence times and substitution rates. We used the programs BEAST 1.4.8 and Tracer (Drummond and Rambaut, 2007), which do not assume autocorrelation, and MULTIDIVTIME (Thorne et al., 1998; Kishino et al., 2001, Thorne and Kishino, 2002), which does.

For the BEAST analysis of the *rbcL* data set, the model parameters determined as optimal by AIC (see results) under the GTR+Γ+I model and suggested priors taken from a prerun analysis were used. A relaxed clock model with an uncorrelated log-normal rate change was chosen. We tuned the operators using BEAST's auto-optimization option. We then executed two runs of 10^7 generations each, sampling every 10^3 generations, using random starting trees, and setting the coalescent process and a speciation model following a Yule process as tree prior. For all BEAST analyses, resulting posterior distributions for parameter estimates were checked in Tracer 1.4.1 (Drummond and Rambaut, 2007), and maximum credibility trees, representing the maximum a posteriori topology, were calculated after removing burn-in with the program TreeAnnotator version 1.4.7. The .xml files are available for the Rutaceae analysis as Appendix S1 and for the *Thamnosma* analysis as Appendix S2 (online at http://www.amjbot.org/cgi/content/full/ajb.1000339/DC1).

For the MULTIDIVTIME analyses, we followed the procedure outlined by Thiv et al. (2006) and a step-by-step manual by Rutschmann (2004). Model parameters for the F84+Γ model (Kishino and Hasegawa, 1989) were estimated using the module BASEML in the program PAML (Yang, 1997). We estimated the maximum likelihood of the branch lengths of the rooted evolutionary tree together with a variance–covariance matrix of the branch length estimates by using the program ESTBRANCHES (Thorne et al., 1998). We used MULTIDIVTIME to approximate the posterior distributions of substitution rates and divergence times by using a multivariate normal distribution of estimated branch lengths (provided here by ESTBRANCHES) and running the MCMC procedure with the following settings for the prior distributions: 1.50 for both *rttm* and *rttmsd*, 0.07 for both *rtrate* and *rtratesd*, 0.4 for both *brownmean* and *brownsd*, and 84 million years ago (Ma) for *bigtime*, which is the maximum age of Sapindales according to Wikström et al. (2001). This maximum age means that this node cannot be estimated to be older than this date. We ran the Markov chain for at least 10^3 cycles and collected one sample every 10^2 cycles, after an unsampled burn-in of 10^4 cycles. We repeated the analyses in BEAST and MULTIDIVTIME twice using different random starting number to assure convergence of the Markov chain and combined the results.

The rate-corrected tree was calibrated with two fossil taxa. A continuous macrofossil record starting form the Late Eocene/Early Oligocene (40–35 Ma) is available for *Euodia* J.R.Forst. & G.Forst. and *Zanthoxylum* L. (Gregor, 1989). Because the macrofossils can be exclusively attributed to these genera (Gregor, 1978, 1989; Tiffney, 1980; Mai, 1995), both were used as calibration points for our age estimates. The oldest known records of *Euodia* and *Zanthoxylum* date from the Late Eocene (35 Ma) and were treated as minimum ages for the stem of the corresponding lineages in the *rbcL* analysis (Fig. 2). For the BEAST analysis, we modeled the clades including *Euodia* and *Zanthoxylum*, each, as an exponential distribution (Ho and Philips, 2009) with a mean of 16.4 and an offset of 35 Ma, which corresponds to the maximum age of these fossils. With this mean value, the 95% distribution covered 84 Ma, which was regarded as big time in the MULTIDIVTIME analysis.

Because *rbcL* was availabile only for a limited number of species, we used the age estimates for some nodes of the *rbcL* tree for a BEAST analysis of the combined ITS/*matK*/*atpB-rbcL* spacer data set including all *Thamnosma* species. This procedure followed the BEAST analysis for *rbcL* with the following specifications. Mean age estimates with standard deviations of the *rbcL* BEAST analysis (nodes b and d in Table 3) served as calibration points under a normal distribution. The GTR+Γ+I model was chosen. We then executed two runs of 10^8 generations each and sampled every 10^4 generations.

Biogeographic analyses—We defined the following areas of endemism for *Thamnosma*: N = North/Central America, H = Horn of Africa including Socotra and Somalia, and S = Southern Africa (Table 1). The outgroup, *Ruta chalepensis*, was coded as Mediterranean, and we did not take into account the potential Asian relatives (see Materials and Methods: Taxon sampling). To reconstruct the geographical evolution of *Thamnosma*, we conducted a dispersal—vicariance analysis (Ronquist, 1997) using the program S-DIVA 1.9 (Yu et al., 2010). This method calculates the optimized areas over a set of trees, thus taking into account topological uncertainty. We used the 9000 trees retained from the BEAST analysis of the combined data set. The number of maximum areas was set to three because this reflects the ingroup's number of defined areas of distribution. To take into account the estimated time between speciation events, we also used the program Lagrange 2.0.1 (Ree and Smith, 2008) for the reconstruction of

ancestral areas, using an ultrametric tree combining the ML topology with internal node age estimates from a BEAST analysis based on the combined data set (not shown). All combinations of areas were allowed in the adjacency matrix, and baseline rates of dispersal and local extinction were estimated.

RESULTS

Rutaceae phylogeny—The aligned sequence lengths of *rbcL* were 811 bp. The optimal model of sequence evolution for this data set was the transversion (TVM+I+Γ) model: unequal base frequencies (A = 0.2721, C = 0.2039, G = 0.2442, T = 0.2798), six substitution types (A/C: 1.5287, A/G: 2.7801, A/T: 0.5796, C/G: 0.9464, C/T: 2.7801), gamma distribution of rates among sites with alpha shape parameter = 0.7607, and the proportion of invariable sites = 0.6326. The analysis using these parameters yielded a ML tree with a log-likelihood score of –lnL = 2962.76. According to the ML tree (Fig. 2), *Thamnosma* is highly supported as monophyletic (99% bootstrap value), and the position as sister to the Mediterranean *Ruta* is supported by a 75% bootstrap value. In the *rbcL* study, both genera appear weakly supported as sister to the Californian *Cneoridium*. Interspecific relationships of *Thamnosma* inferred from a reduced taxon sample were partly resolved by *rbcL* data. Except for the position of *T. trifoliata*, they correspond to the results of the second, more detailed analysis reported next.

Thamnosma phylogeny—The aligned sequence lengths were 224 bp (ITS1), 231 bp (ITS2), 664 bp (*matK*), and 994 bp (*atpB-rbcL* spacer), resulting in a total length of 2113 bp, of which 0.89% were scored as missing data. Of these characters, 248 were variable and 62 parsimony informative. A partition homogeneity test explained incongruence between the nuclear and chloroplast data at $P = 0.954$. Therefore, we combined the data sets. The MP analysis yielded a single most parsimonious tree with a length of 306 steps, a CI of 0.92 and a RI of 0.80. The optimal model of sequence evolution for this combined data set was the general time reversible (GTR+I+Γ) model: unequal base frequencies (A = 0.2793, C = 0.2042, G = 0.2169, T = 0.2996) and six substitution types (A/C: 1.0607, A/G: 1.4094, A/T: 0.3057, C/G: 1.3575, C/T: 3.0006), gamma distribution of rates among sites with alpha shape parameter = 0.6826, and the proportion of invariable sites = 0.5533. The analysis using these parameters yielded a ML tree with a log-likelihood score of –lnL = 4667.27.

The MP, ML, and Bayesian analyses, all indicate that the North American species are paraphyletic relative to the Old World taxa (Figs. 3, 4). All analyses recognize a North American clade consisting of *T. stanfordii*, *T. pailensis*, and *T. texana* and a palaeotropical lineage including *T. africana*, *T. crenata*, *T. rhodesica*, *T. somalensis*, *T. hirschii*, and *T. socotrana*. This latter clade is subdivided into the southern African *T. africana-T. crenata-T. rhodesica*, and the Eastern African-Arabian-Socotran *T. socotrana-T. somalensis-T. hirschii*. The results differ with regard to the positions of *T. trifoliata* and *T. montana*. In the MP study, *T. montana* is sister to the rest of the genus, and *T. trifoliata* appears as sister to *T. stanfordii-T. pailensis-T. texana*. The ML tree places *T. trifoliata* at the base, followed by *T. stanfordii-T. pailensis-T. texana* and *T. montana* as sister to the Old World clade. The Bayesian analysis does not resolve relationships between *T. trifoliata*, *T. stanfordii-T. pailensis-T. texana*, but also indicates *T. montana* is sister to the palaeotropical group. The relationships between these North American lineages are only weakly supported in all analyses, showing bootstrap values (BS) or posterior probabilities (PP) < 53%.

The alternative hypotheses of all northern American species forming a clade and of *T. socotrana-T. somalensis* being sister to each other resulted each in a difference of tree length of two steps in the parametric bootstrap analysis. While the first alternative cannot be rejected at $P > 0.05$, the second one is dismissed at $P = 0.04$.

Molecular dating—Enforcing the molecular clock resulted in a log-likelihood score of −lnL = 2989.19 for the *rbcL* data set. The comparison between clock and nonclock (LR = −3356.16) trees by applying the likelihood ratio (LR) test did not reject clock-like evolution for this data set (df = 36, $P < 0.05$). The results of the two runs using BEAST were very similar and were therefore combined. The same applied to the two runs using MULTIDIVTIME. The estimated mean ages and 95% highest posterior density intervals (HPD) are shown in Table 3 referring to nodes of a clock-like ML tree in Fig. 2. For the *rbcL* data set, the mean substitution rate as indicated by Tracer is 2.96×10^{-10} substitution·site^{-1}·yr^{-1}. The ages of the dated lineages inferred by BEAST are generally older than those by MULTIDIVTIME. Nonetheless, there is a broad overlap in HPD between the outcomes of the two programs. The consensus tree of the BEAST analysis of all *Thamnosma* species is shown in Fig. 4. Most important for our considerations are the following nodes (Table 3). The largest divergence is found for of the stem group of *Thamnosma* with mean values of 36.75 (14.66–61.55) Ma using BEAST and 22.25 (9.21–34.92) Ma as calculated by MULTIDIVTIME. The mean estimated age of the crown node of *Thamnosma* is 14.56 Ma (4.78–26.35) and 13.11 (3.33–26.83), respectively. The average age of the split between New and Old World *Thamnosma* was calculated as 12.63 (8.37–14.94, node F in Table 3) Ma. The age of the southern African and Horn of Africa clade is 8.53 (5.28–12.11, node E in Table 3) Ma. Divergence between Socotran *T. socotrana* and east African-Arabian(-Socotran) *T. hirschii* was determined to be 5.15 (0.36–11.38) and 4.09 (0.13–13.65, node D/d in Table 3) Ma.

Biogeography—The results of Lagrange and DIVA analyses are given in Table 4 in which nodes refer to those in Figs. 3 and 4. Using the the ML tree, we optimized the two most basal nodes (B and G) with the splits N|NH, N|NS, and N|N in Lagrange and mostly with N as ancestral area in S-DIVA. The lineage of *T. montana* and the Old World yielded almost equally likely N|H and N|S, and NH, NS, and NHS. Within the palaeotropical clade, Lagrange and DIVA clearly indicate a split between S and H.

DISCUSSION

***Phylogeny of* Thamnosma**—Our *rbcL* data support the monophyly of *Thamnosma* and its close relationship to *Ruta* and *Cneoridium*, thus corroborating the results of Salvo et al. (2008). The palaeotropical species of *Thamnosma* form a strongly supported clade, which contains two subclades: a southern African and a eastern African-Arabian-Socotran subclade. Beside high BS and PP values, the occurrence of segmented leaves also supports the southern African clade. No morphological synapomorphy could be found for the eastern African-Arabian-Socotran clade.

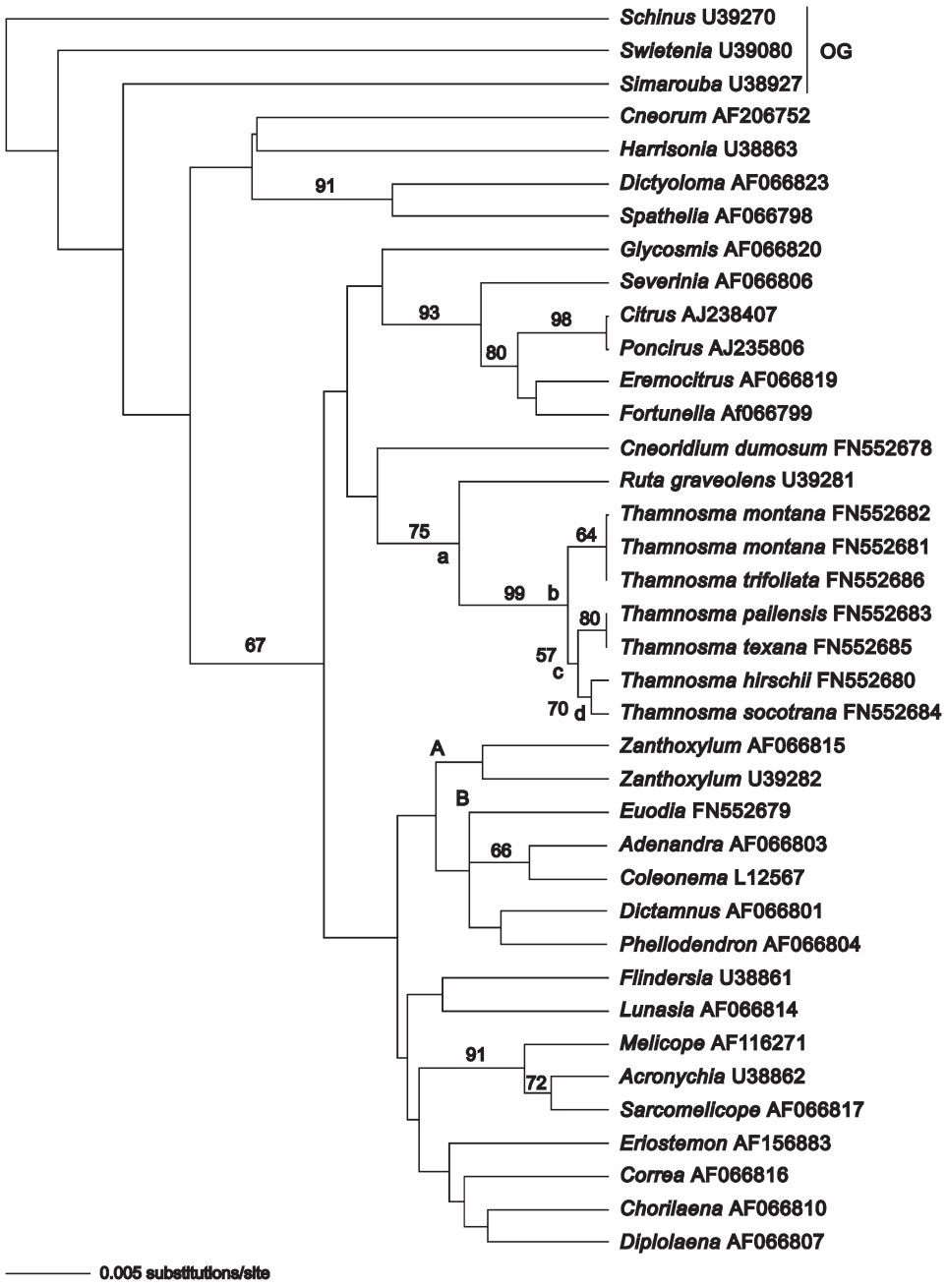

Fig. 2. Clock-like maximum likelihood (ML) tree of selected Rutaceae based on *rbcL* sequences. Capitals A and B indicate calibration points. Lowercase letters a–d refer to nodes in Table 3. ML bootstrap values (>50%) are on the branches. Numbers behind taxon names refer to EMBL accession numbers (Table 2).

The three species differ mainly in growth form and in quantitative traits like petal, fruit, and seed lengths. The sister-group relationship between *T. somalensis* and *T. hirschii* is supported by high bootstrap and PP values. The alternative relationship of *T. somalensis* as sister to *T. socotrana*, proposed by Thulin (1999), is not corroborated by our data and is rejected by the parametric bootstrap analysis. The palaeotropical clade appears to be nested within North American species. The phylogenetic relationships among the North American species remain ambiguous, and no single topology is well supported (Fig. 3). Furthermore, the monophyly of the North American species cannot be ruled out by parametric bootstrap analysis. The only well-supported relationship is the sister-species relationship between *T. pailensis* and *T. texana*, which is morphologically corroborated by the possession of yellow petals (Johnston, 1983). The different positions of *T. trifoliata* and *T. montana* might hint at low DNA divergence, ancient hybridization events or long branch attraction. Here we assume that the weakly supported paraphyly of the North American *Thamnosma* species relative to the Old World ones is correct.

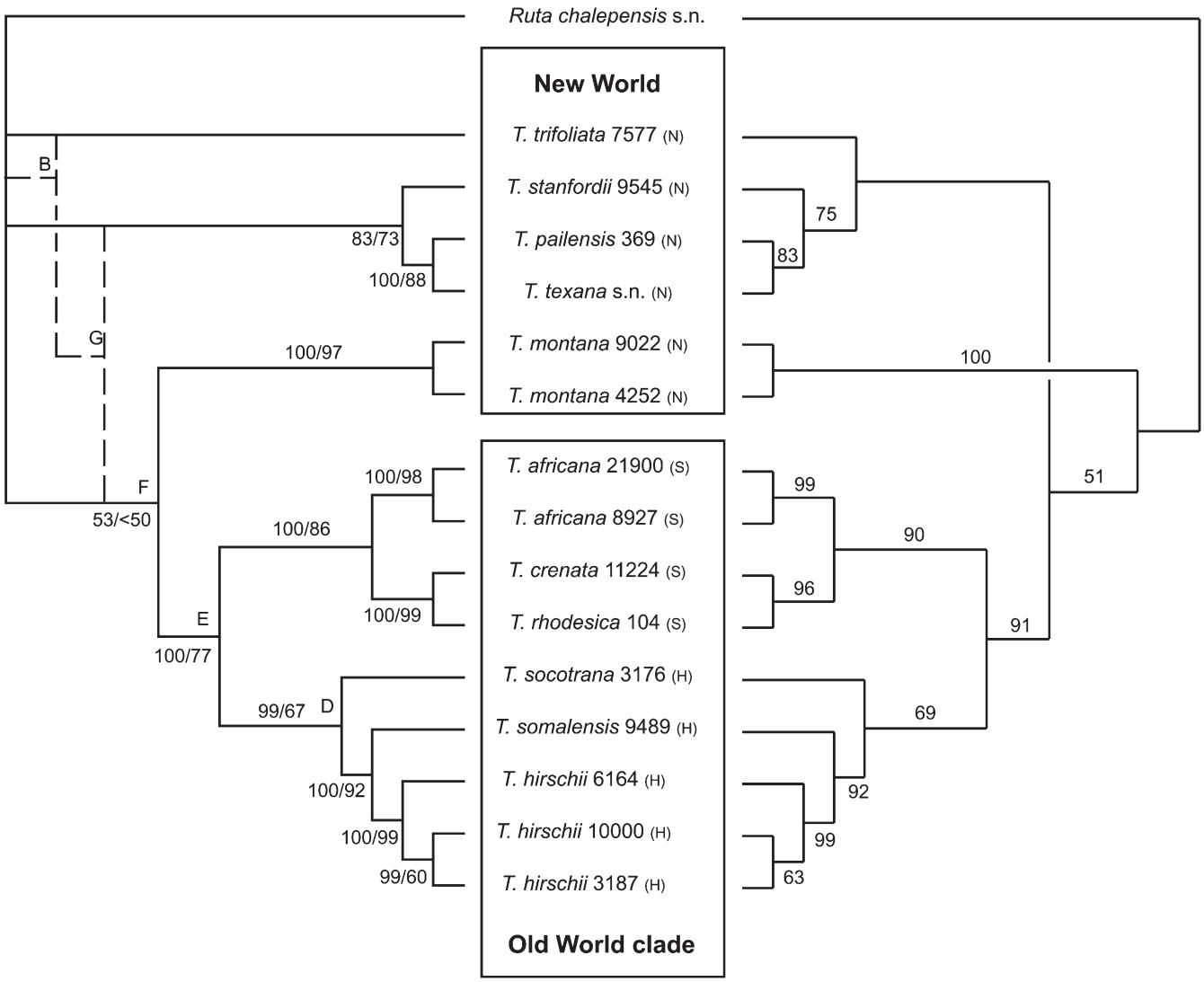

Fig. 3. Phylogenetic reconstructions of *Thamnosma* based on nrITS, *matK*, and *atpB-rbcL* intergenic spacer sequences. Left is shown the almost identical cladogram of the Bayesian and maximum likelihood (ML) analyses. ML resolves the positions of *T. trifoliata* and *T. stanfordii-T. pailensis/T. texana* as indicated by the bracked line. Posterior probabilities and ML bootstrap values (>50%) are in this order on the branches. Single MP tree is shown on the right including bootstrap values. For detailed species distribution, see Table 1. *T.* = *Thamnosma*. Numbers behind species names refer to collection numbers as shown in Table 2. Capitals B and D–G refer to nodes in Tables 3 and 4.

Is* Thamnosma *a member of the Madro-Tertiary geoflora?—Axelrod (1958) described a Madro-Tertiary geoflora, which was widespread in North America since the Eocene–Oligocene boundary (34 Ma). Members of this flora were characterized by sclerophyllous, microphyllous leaves, which also suggested an arid, warm climate. Despite the fact that the leaves of *Thamnosma* are nanophyllous and deciduous, the ecology is still consistent with it being a member of the Madro-Tertiary geoflora. The present distribution of the North American *Thamnosma* in southwestern North America corresponds largely with the center of the Madro-Tertiary geoflora. All these taxa grow in arid-adapted vegetation (Johnston, 1924, 1943, 1983). Further evidence comes from the association of extant *Thamnosma* with taxa listed by Axelrod (1958) as elements of the Madro-Tertiary geoflora, suggesting that *Thamnosma*, despite the absence of fossils, may have been part of the Madro-Tertiary geoflora. Alternatively, *Thamnosma* may have evolved outside the Madro-Tertiary geoflora and later migrated into its modern distribution range in the southern United States and Mexico. If the present North American *Thamnosma* are relictual elements of the Madro-Tertiary geoflora, then we predict that the time of radiation of North American *Thamnosma* coincides with the period of the Madro-Tertiary geoflora, about 34–2 Ma.

According to our molecular clock calculations, the stem group age of *Thamnosma* is either about 22 Ma (9.2–34.9) using MULTIDIVTIME or 36.8 Ma (14.7–61.6) using BEAST. These ages may be overestimated because *Boenninghausenia* and *Psilopeganum* may break up this branch. Both age estimates of *Thamnosma* correspond to the time when the Madro-Tertiary geoflora was expanding in the Miocene (Axelrod, 1958; Graham, 1999). The radiation of the North American *Thamnosma* started around 13–15 (3.3–26.8) Ma (node b in Fig. 2, Table 3). Thus, our

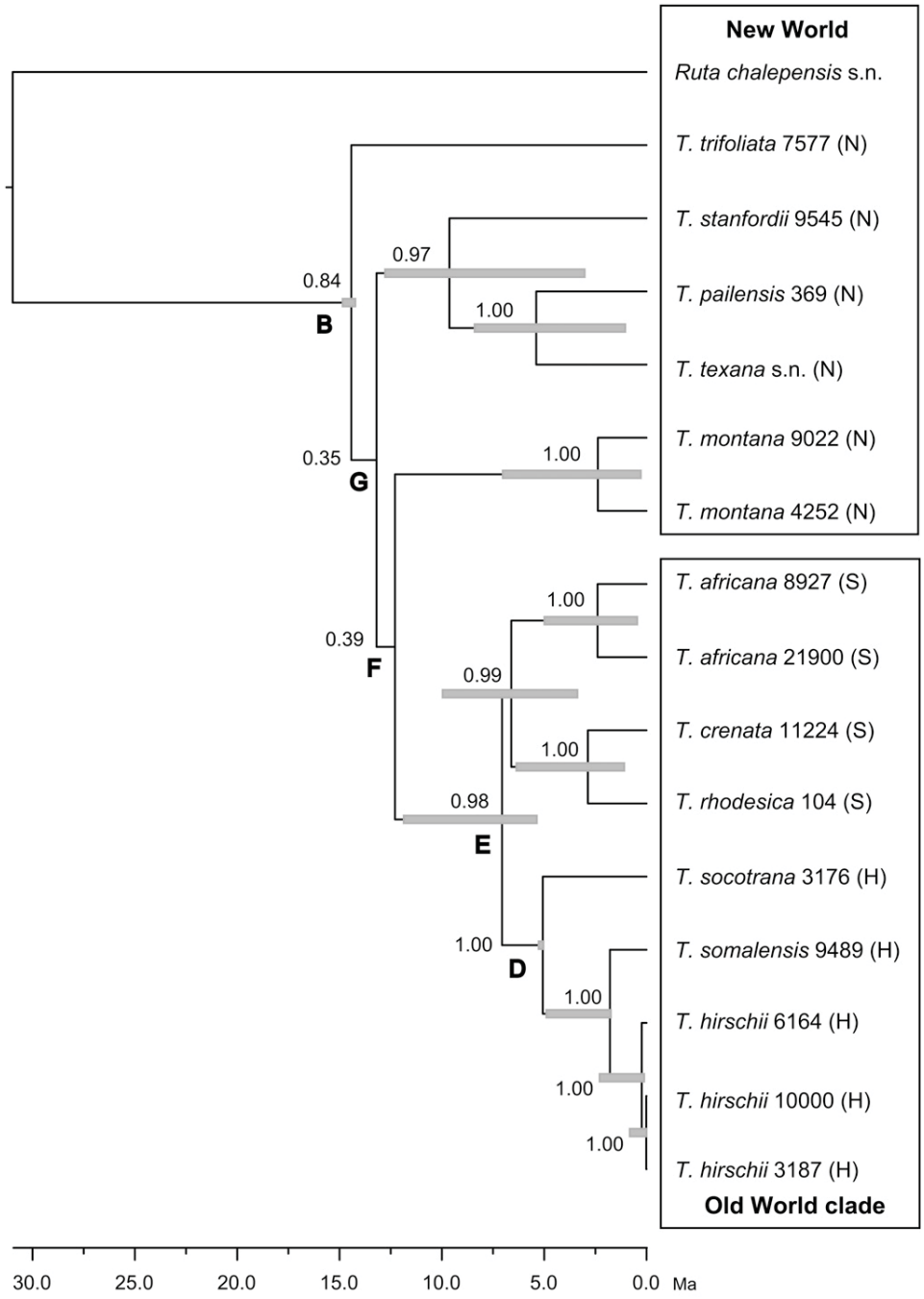

Fig. 4. Chronogram of *Thamnosma* of the Bayesian dating analysis using BEAST. Posterior probability values are shown at nodes. Gray bars indicate 95% highest posterior density (HPD) of age estimates. Other features as in Fig. 3.

results are consistent with an early radiation of *Thamnosma* in the Madro-Tertiary geoflora, i.e., the ancestors of the extant species may have been part of this flora. If the east Asian *Psilopeganum* and/or *Boenninghausenia* are the closest relatives of *Thamnosma*, an origin of the North American species from the Neotropics or an Arcto-Tertiary stock (Axelrod, 1958), as suggested for *Rhus* L. (Anacardiaceae) by molecular data (Miller et al., 2001), can be ruled out. More plausible are connections to tropical to subtropical Asia supporting the boreotropics hypothesis postulating links between the North American and Asian Eocene floras (Wolfe, 1975; Lavin and Luckow, 1993), possibly via the Beringian land bridge.

New–Old World disjunctions in the succulent biome flora—Our data enable us to test two hypotheses on the origin of North American and Eurasian–African disjunctions of taxa of the succulent biome. First, vicariance hypotheses predict that the age of the disjunction should match the age of the land connections between the two continents: these may even be sorted

TABLE 3. Results of the Bayesian dating using BEAST and MULTIDIVTIME showing combined mean ages and the 95% highest posterior density (HPD) of two runs. Nodes in lowercase letters refer to Fig. 2 and those in capital letters to Figs. 3 and 4.

	BEAST			MULTIDIVTIME	
Node	Mean (Ma)	95% HPD (Ma)	SE	Mean (Ma)	95% HPD (Ma)
a	36.75	14.66-61.55	0.38	22.25	9.21–34.92
b/B	14.56	4.78-26.35	0.16	13.11	3.33–26.83
c	10.52	2.80-20.43	1.12	8.60	1.22–20.96
d/D	5.15	0.36-11.38	0.06	4.09	0.13–13.65
E	8.53	5.28-12.11	0.02	—	—
F	12.63	8.37-14.94	0.03	—	—

by the age of the last connection (North Atlantic or Beringia). Second, long-distance dispersal is the most likely explanation when all vicariance patterns can be rejected.

The vicariance hypotheses cannot be so easily rejected. The estimated age of the split between the American and the African taxa in the Miocene (12.63, 8.37–14.94 Ma, node F in Table 3) falls outside the time frames of both Axelrod's (1975) Madrean-Tethyan (37.2–23 Ma) and Tiffney's (1985b) Eocene North Atlantic land bridge (55.8–33.9 Ma) hypotheses. This is inconsistent with vicariance across the North Atlantic, and these results are congruent with those of Lavin et al. (2004) for legumes and Hohmann et al. (2006) for the Californian–Mediterranean *Aphanisma–Oreobliton* (Amaranthaceae) disjunction. Moreover, the Madrean-Tethyan hypothesis referred to the Mediterranean area rather than the succulent biome in the strict sense of Schrire et al. (2005a). Our age estimates cannot reject vicariance across an early Miocene (23–16 Ma) migration route via the Bering land bridge (Stebbins and Day, 1967; Tiffney, 1985a; Hohmann et al., 2006). The much larger distance between North America and Africa via Beringia and the absence of *Thamnosma* in Asia argue against it (cf. Hohmann et al., 2006). It is possible, though unlikely, that the succulent biome, with *Thamnosma* in it, may have existed undetected in Asia during the Neogene. Consequently a vicariance explanation for the disjunction is unlikely.

Because the vicariance hypotheses are unlikely, we are left with the long-distance dispersal hypothesis. Numerous cases of long-distance dispersal from North America to Africa during the Miocene have been postulated, based on African clades nested in a paraphyletic American assemblage of taxa. Examples can be found in the legumes (Lavin et al., 2004) and in *Acleisanthes* A. Gray incl. *Selinocarpus* A. Gray (Nyctaginaceae, Levin, 2000, 2002) where a single Somalian species is nested within the American clade of 15 species. We regard this explanation as the most likely one for this disjunction.

TABLE 4. Results of the biogeographic reconstructions using Lagrange and S-DIVA. Abbreviations and nodes refer to Figs. 3 and 4.

	Lagrange			S-DIVA	
Node	Split	-lnL	Relative probability	Ancestral area	Frequency (%)
B	[N|NH]	16.66	0.41	N	56.4
	[N|NS]	16.67	0.40	NS	14.6
	[N|N]	17.47	0.18	NHS	14.5
				NH	14.5
E	[S|H]	15.83	0.93	SH	99.9
				H	0.1
				S	0.1
F	[N|H]	16.50	0.48	NHS	34.1
	[N|S]	16.51	0.47	NH	33.0
				NS	33.0
G	[N|NH]	16.58	0.44	N	77.8
	[N|NS]	16.59	0.43	NHS	7.4
	[N|N]	17.85	0.12	NS	7.4
				NH	7.4

African patterns—*Thamnosma* radiated in southern and northeast Africa, giving rise to two geographically separated clades (node E in Table 4). These six species map a track that connects the arid regions of southwestern Africa (Namibia, Botswana, the northern parts of South Africa) with those of northeastern Africa (Kenya, Somalia, Ethiopia). This "arid corridor" has been documented for many plant groups (Balinsky, 1962; Verdcourt, 1969; de Winter, 1971; Jürgens, 1997). The age of this corridor, specifically the time of its initiation and also closure, is disputed. Some estimates date it to the Pleistocene, thus linking it to the glacial–interglacial Pleistocene cycles. Other estimates suggest a Miocene date and a severance of the corridor due to Late Miocene uplift and associated rifting in Africa (Chorowicz, 2005) or major climatic changes during the Late Miocene (Schuster et al., 2006; Bobe, 2006). The age of the diversification between the southern African and northeast Africa clades of *Thamnosma* is in the Lower Miocene (8.53 [5.28–12.11] Ma, Table 3). This coincides with the age estimates of corresponding lineages of *Androcymbium* (Caujape-Castells et al., 2001) and supports Balinsky's (1962) suggestion that the arid corridor existed already before the Pleistocene, not ruling out repeated openings and closures in different periods. However, the possibility that the distribution range was established by long-distance dispersal, and not by migration through the arid corridor, cannot be discounted by our data.

Thamnosma socotrana, an endemic of the Haggeher mountains on Socotra (Miller and Morris, 2004), is basal in the east African clade. Although today geographically closer to the Horn of Africa, the Socotran archipelago was separated from the Arabian peninsula 18–15 Ma (Richardson et al., 1995; Fleitmann et al., 2004; Van Damme, 2009). Both vicariance and long-distance dispersal have been proposed as explanations for the source of the Socotran endemics (Mies, 2001; Miller and Morris, 2004). A vicariance explanation for the presence of *T. socotrana* on the island predicts that the species should have separated from its nearest continental relatives at least 18 Ma. The Upper Miocene-Pleistocene date (node d/D in Table 3) for the separation of *T. socotrana* from the other two species of the East African clade clearly falsifies the vicariance hypothesis. Our estimated date is in accordance with other recent studies focusing on Socotra (Lavin et al., 2000; Thulin and Lavin, 2001; Thiv et al., 2006; 2010), showing that most of the flora arrived by long-distance dispersal.

Niche conservation—All species of *Thamnosma* are restricted to dry environments as defined by Köppen (Peel et al., 2007) and specifically to the succulent biome (Schrire et al., 2005a). The small (nano- and leptophyllous) deciduous leaves most likely constitute an adaptation to this seasonally arid climate. In concordance with our age estimates, the presence of semiarid conditions in North America in the Middle Miocene (Axelrod, 1958) served as source of a preadapted aridland Old world lineage. On a local scale, however, there is some differentiation visible. As discussed by Lavin et al. (2004) and Pennington et al. (2009), the arid biome is characterized globally by highly isolated regions, and consequently most species

are narrow endemics. *Thamnosma* seems to parallel the patterns found for legumes. Only *T. texana* and *T. montana* are more widespread in the southern United States and Central America, all other species occur allopatrically in very restricted areas (Table 1). Among the eastern African species, *T. hirschii* grows in several vegetation types from semidesert open grass land to evergreen bushland at altitudes between 10–1500 m a.s.l. The remaining two species occupy much narrower, montane habitats that mainly differ in their substrate. *Thamnosma socotrana* is found on granite, while *T. somalensis* is known from limestone slopes (Thulin, 1999). Some differentiation can also be observed in the southern African lineage. Here, *T. africana* and *T. rhodesica* prefer dry bushland and rock crevices, while *T. crenata* extends its habitat to grasslands (Thulin, 1999).

The genus does not penetrate in Africa into the more mesic savannas (e.g., the Central African Miombo or the West African savannas), nor into the rainforests of the Congo basin or the East African coast. It is also absent from the cooler and more mesic evergreen forests and temperate grasslands of the African uplands, which are widespread from Malawi to Ethiopia along the African rift valley system. Because all species in the genus share this ecology (the combination of which habitats are actually occupied, and from which it is missing), this pattern can be interpreted as a phylogenetic niche conservatism. A direct result of this conservatism is the fragmented distribution in Africa.

Conclusion—The diversity of *Thamnosma* may be the result of three processes: phylogenetic niche conservatism, rare long-distance dispersal, and local differentiation. The first constrains the genus to the succulent biome, the second allows occupation of these geographically separated regions, without genetically swamping locally differentiating lineages, and the last allows the evolution of local specialist species. The result is a global succulent biome, with many shared genera or clades but a few shared species.

LITERATURE CITED

AXELROD, D. I. 1958. Evolution of the Madro-Tertiary geoflora. *Botanical Review* 24: 433–509.

AXELROD, D. I. 1972. Edaphic aridity as a factor in angiosperm evolution. *American Naturalist* 106: 311–320.

AXELROD, D. I. 1973. History of the Mediterranean ecosystem in California. *In* F. di Castri and H. A. Mooney [eds.], Mediterranean type ecosystems—Origin and structure, 225–277. Springer Verlag, Berlin, Germany.

AXELROD, D. I. 1975. Evolution and biogeography of Madrean-Tethyan sclerophyll vegetation. *Annals of the Missouri Botanical Garden* 62: 280–334.

BALINSKY, B. I. 1962. Patterns of animal distribution on the African continent. *Annals of the Cape Provincial Museum* 2: 299–310.

BELLSTEDT, D. U., L. VAN ZIJL, E. M. MARAIS, B. BYTEBIER, C. A. DE VILLIERS, A. M. MAKWARELA, AND L. L. DREYER. 2008. Phylogenetic relationships, character evolution and biogeography of southern African members of *Zygophyllum* (Zygophyllaceae) based on three plastid regions. *Molecular Phylogenetics and Evolution* 47: 932–949.

BLATTNER, F. R. 1999. Direct amplification of the entire ITS region from poorly preserved plant material using recombinant PCR. *BioTechniques* 27: 1180–1186.

BOBE, R. 2006. The evolution of arid ecosystems in eastern Africa. *Journal of Arid Environments* 66: 564–584.

CAUJAPÉ-CASTELLS, J., R. K. JANSEN, N. MEMBRIVES, J. PEDROLA-MONFORT, J. M. MONTSERRAT, AND A. ARDANUY. 2001. Historical biogeography of *Androcymbium* Willd.(Colchicaceae) in Africa: Evidence from cpDNA RFLPs. *Botanical Journal of the Linnean Society* 136: 379–392.

CHOROWICZ, J. 2005. The East African Rift system. *Journal of African Earth Sciences* 43: 379–410.

COLEMAN, M., A. LISTON, J. W. KADEREIT, AND R. J. ABBOTT. 2003. Repeat intercontinental dispersal and Pleistocene speciation in disjunct Mediterranean and desert *Senecio* (Asteraceae). *American Journal of Botany* 90: 1446–1454.

CRISP, M. D., M. T. K. ARROYO, L. G. COOK, M. A. GANDOLFO, G. J. JORDAN, M. S. MCGLONE, P. H. WESTON, ET AL. 2009. Phylogenetic biome conservatism on a global scale. *Nature* 458: 754–756.

DA SILVA, M. F. D. G. F., O. R. GOTTLIEB, AND F. EHRENDORFER. 1988. Chemosystematics of the Rutaceae: Suggestions for a more natural taxonomy and evolutionary interpretation of the family. *Plant Systematics and Evolution* 161: 97–134.

DE WINTER, B. 1971. Floristic relationships between the northern and southern arid areas in Africa. *Mitteilungen der botanischen Staatssammlung München* 10: 424–437.

DONOGHUE, M. J. 2008. A phylogenetic perspective on the distribution of plant diversity. *Proceedings of the National Academy of Sciences, USA* 105: 11549–11555.

DRUMMOND, A. J., AND A. RAMBAUT. 2007. BEAST: Bayesian evolutionary analysis by sampling trees. *BMC Evolutionary Biology* 7: 214.

ENGLER, A. 1897. Rutaceae. *In* A. Engler and K. Prantl [eds.], Die natürlichen Pflanzenfamilien, 95–201. Wilhelm Engelmann, Leipzig, Germany.

ENGLER, A. 1931. Rutaceae. *In* A. Engler and H. Harms [eds.], Die natürlichen Pflanzenfamilien, 187–359. Wilhelm Engelmann, Leipzig, Germany.

FELSENSTEIN, J. 1981. Evolutionary trees from DNA sequences: A maximum likelihood approach. *Journal of Molecular Evolution* 17: 368–376.

FLEITMANN, D., A. MATTER, S. J. BURNS, A. AL-SUBBARY, AND M. A. AL-AOWAH. 2004. Geology and Quaternary climate history of Socotra. *Fauna of Arabia* 20: 27–43.

FREITAG, S., AND T. J. ROBINSON. 1993. Phylogeographic patterns in mitochondrial DNA of the ostrich (*Struthio camelus*). *Auk* 110: 614–622.

GOLDMAN, N., J. P. ANDERSON, AND A. G. RODRIGO. 2000. Likelihood-based tests of topologies in phylogenetics. *Systematic Biology* 49: 652–670.

GRAHAM, A. 1999. Late Cretaceous and Cenozoic history of North American vegetation. Oxford University Press, New York, New York, USA.

GREGOR, H. J. 1978. Subtropische Elemente im europäischen Tertiär III Rutaceae Die Gattungen *Toddalia* und *Zanthoxylum. Acta Palaeobotanica* 19: 21–40.

GREGOR, H. J. 1989. Aspects of the fossil record and phylogeny of the family Rutaceae (Zanthoxyleae, Toddalioideae). *Plant Systematics and Evolution* 162: 251–265.

HO, S. Y. W., AND M. J. PHILIPS. 2009. Accounting for calibration uncertainty in phylogenetic estimation of evolutionary divergence times. *Systematic Biology* 58: 367–380.

HOHMANN, S., J. W. KADEREIT, AND G. KADEREIT. 2006. Understanding Mediterranean–Californian disjunctions: Molecular evidence from Chenopodiaceae-Betoideae. *Taxon* 55: 67–78.

HUELSENBECK, J. P., D. M. HILLIS, AND R. JONES. 1996. Parametric bootstrapping in molecular phylogenies: Application and performance. *In* J. D. Ferris and S. R. Palumbi [eds.], Molecular zoology: Advances, strategies, and protocols, 19–45. Wiley, New York, New York, USA.

HUELSENBECK, J. P., AND F. RONQUIST. 2001. MrBayes: Bayesian inference of phylogeny. *Bioinformatics* 17: 754–755.

JOHNSON, L. A., AND D. E. SOLTIS. 1998. Assessing congruence: Empirical examples from molecular data. *In* D. E. Soltis, P. S. Soltis, and J. J. Doyle [eds.], Molecular systematics of plants II: DNA sequencing, 297–348. Kluwer, New York, New York, USA.

JOHNSTON, I. M. 1924. Expedition of the Californian Academy of Sciences to the Gulf of California in 1921: The botany (the vascular plants). *Proceedings of the California Academy of Sciences, series 4* 12: 951–1218.

JOHNSTON, I. M. 1943. Noteworthy species from Mexico and adjacent United States, I. *Journal of the Arnold Arboretum* 24: 227–236.

JOHNSTON, M. C. 1983. *Thamnosma pailensis* (Rutaceae), new species from the Sierra de la Paila, Coahuila Mexico. *Phytologia* 53: 179–180.

JÜRGENS, N. 1997. Floristic biodiversity and history of African arid regions. *Biodiversity and Conservation* 6: 495–514.

KISHINO, H., AND M. HASEGAWA. 1989. Evaluation of the maximum likelihood estimate of the evolutionary tree topologies from DNA sequence data, and the branching order in Hominoidea. *Journal of Molecular Evolution* 29: 170–179.

KISHINO, H., J. L. THORNE, AND W. J. BRUNO. 2001. Performance of a divergence time estimation method under a probabilistic model of rate evolution. *Molecular Biology and Evolution* 18: 352–361.

LAVIN, M., AND M. LUCKOW. 1993. Origins and relationships of tropical North America in the context of the boreotropics hypothesis. *American Journal of Botany* 80: 1–14.

LAVIN, M., M. THULIN, J. N. LABAT, AND R. T. PENNINGTON. 2000. Africa, the odd man out: Molecular biogeography of dalbergioid legumes (Fabaceae) suggests otherwise. *Systematic Botany* 25: 449–467.

LAVIN, M., B. P. SCHRIRE, G. LEWIS, R. T. PENNINGTON, A. DELGADO-SALINAS, M. THULIN, C. E. HUGHES, ET AL. 2004. Metacommunity process rather than continental tectonic history better explains geographically structured phylogenies in legumes. *Philosophical Transactions of the Royal Society of London, B, Biological Sciences* 359: 1509–1522.

LEVIN, R. A. 2000. Phylogenetic relationships within Nyctaginaceae Tribe Nyctagineae: Evidence from nuclear and chloroplast genomes. *Systematic Botany* 25: 738–750.

LEVIN, R. A. 2002. Taxonomic status of *Acleisanthes, Selinocarpus*, and *Ammocodon* (Nyctaginaceae). *Novon* 12: 58–63.

MACEY, J. R., J. V. KUEHL, A. LARSON, M. D. ROBINSON, I. H. UGURTAS, N. B. ANANJEVA, H. RAHMAN, ET AL. 2008. Socotra Island the forgotten fragment of Gondwana: Unmasking chameleon lizard history with complete mitochondrial-genomic data. *Molecular Phylogenetics and Evolution* 49: 1015–1018.

MAI, D. H. 1995. Tertiäre Vegetationsgeschichte Europas—Methoden und Ergebnisse. Gustav Fischer Verlag, Jena, Germany.

MANEN, J.-F., A. NATALI, AND F. EHRENDORFER. 1994. Phylogeny of Rubiaceae-Rubieae inferred from the sequence of a cpDNA intergene region. *Plant Systematics and Evolution* 190: 195–211.

MIES, B. A. 2001. Flora und Vegetationsökologie der Insel Soqotra. Westarp Wissenschaften, Hohenwarsleben, Germany.

MILLER, A. G., AND M. MORRIS. 2004. Ethnoflora of the Soqotra Archipelago. RBG Edinburgh, Edinburgh, UK.

MILLER, A. J., D. A. YOUNG, AND J. WEN. 2001. Phylogeny and biogeography of *Rhus* (Anacardiaceae) based on ITS sequence data. *International Journal of Plant Sciences* 162: 1401–1407.

MOONEY, H. A., AND E. L. DUNN. 1970. Convergent evolution of Mediterranean-climate evergreen sclerophyll shrubs. *Evolution* 24: 292–303.

NEI, M., AND S. KUMAR. 2000. Molecular evolution and phylogenetics. Oxford University Press, Oxford, UK.

NYLANDER, J. A. A. 2004. MrModeltest v2. Program distributed by the author, Evolutionary Biology Centre, Uppsala University, Uppsala, Sweden.

PEEL, M. C., B. L. FINLAYSON, AND T. A. MCMAHON. 2007. Updated world map of the Köppen-Geiger climate classification. *Hydrology and Earth System Sciences* 11: 1633–1644.

PENNINGTON, R. T., M. LAVIN, AND A. OLIVEIRA-FILHO. 2009. Woody plant diversity, evolution, and ecology in the tropics: Perspectives from seasonally dry tropical forests. *Annual Review of Ecology Evolution and Systematics* 40: 437–457.

POSADA, D., AND K. A. CRANDALL. 1998. Modeltest: Testing the model of DNA substitution. *Bioinformatics* 14: 817–818.

RAMBAUT, A., AND N. C. GRASSLY. 1997. Seq-Gen: An application for the Monte Carlo simulation of DNA sequence evolution along phylogenetic trees. *Computer Applications in the Biosciences* 13: 235–238.

REE, R. H., AND S. A. SMITH. 2008. Maximum likelihood inference of geographic range evolution by dispersal, local extinction, and cladogenesis. *Systematic Biology* 57: 4–14.

RICHARDSON, S. M., W. F. BOTT, B. A. SMITH, W. D. HOLLAR, AND P. M. BERMINGHAM. 1995. A new hydrocarbon "play" area offshore Socotra Island, Republic of Yemen. *Journal of Petroleum Geology* 77: 225–244.

RONQUIST, F. 1997. Dispersal-vicariance analysis: A new approach to the quantification of historical biogeography. *Systematic Biology* 46: 195–203.

RUTSCHMANN, F. 2004. Bayesian molecular dating using PAML/multidivtime. A step-by-step manual [online]. University of Zurich, Switzerland. Available at ftp://statgen.ncsu.edu/pub/thorne/bayesiandating1.5.pdf [6 December 2010].

SALVO, G., G. BACCHETTA, F. GHAHREMANINEJAD, AND E. CONTI. 2008. Phylogenetic relationships of Ruteae (Rutaceae): New evidence from the chloroplast genome and comparisons with non-molecular data. *Molecular Phylogenetics and Evolution* 49: 736–748.

SANDERSON, M. J. 1998. Estimating rate and time in molecular phylogenies: Beyond the molecular clock? *In* D. E. Soltis, P. S. Soltis, and J. J. Doyle [eds.], Molecular systematics of plants, 242–264. Kluwer, New York, New York, USA.

SANG, T., D. J. CRAWFORD, AND T. F. STUESSY. 1997. Chloroplast DNA phylogeny, reticulate evolution, and biogeography of *Paeonia* (Paeoniaceae). *American Journal of Botany* 84: 1120–1136.

SCHRIRE, B. D., M. LAVIN, N. P. BARKER, AND F. FOREST. 2009. Phylogeny of the tribe Indigofereae (Leguminosae–Papilionoideae): Geographically structured more in succulent-rich and temperate settings than in grass-rich environments. *American Journal of Botany* 96: 816–852.

SCHRIRE, B. D., M. LAVIN, AND G. P. LEWIS. 2005a. Global distribution patterns of the Leguminosae: insights from recent phylogenies. *In* I. Friis and H. Balslev [eds.], Plant diversity and complexity patterns: Local, regional and global dimensions, 375–422. Royal Danish Academy of Sciences and Letters, Copenhagen, Denmark.

SCHRIRE, B. D., G. LEWIS, AND M. LAVIN. 2005b. Biogeography of the Leguminosae. *In* G. Lewis, B. D. Schrire, B. Mackinder, and J. M. Lock [eds.], Legumes of the world, 21–54. Royal Botanic Gardens, Kew, UK.

SCHUSTER, M., P. DURINGER, J. F. GHIENNE, P. VIGNAUD, H. T. MACKAYE, A. LIKIUS, AND M. BRUNET. 2006. The age of the Sahara desert. *Science* 311: 821.

SONG, W.-H., X.-D. LI, X.-W. LI, H.-W. HUANG, AND J.-Q. LI. 2004. Genetic diversity and conservation strategy of *Psilopeganum sinense*, a rare species in the three-gorges reservoir area. *Biodiversity Science* 12: 227–236.

STEBBINS, G. L., AND A. DAY. 1967. Cytogenetic evidence for long continued stability in the genus *Plantago*. *Evolution* 21: 409–428.

STEFANOVIĆ, S., AND R. G. OLMSTEAD. 2004. Testing the phylogenetic position of a parasitic plant (*Cuscuta*, Convolvulaceae, Asteridae): Bayesian inference and the parametric bootstrap on data drawn from three genomes. *Systematic Biology* 53: 384–399.

SWOFFORD, D. L. 1998. PAUP*: Phylogenetic analysis using parsimony (*and other methods), version 4.0. Sinauer, Sunderland, Massachusetts, USA.

TAKHTAJAN, A. 1986. Floristic regions of the world. University of California Press, Berkeley, California, USA.

THIV, M., AND U. MEVE. 2007. A phylogenetic study of *Echidnopsis* Hook. f. (Apocynaceae-Asclepiadoideae): Taxonomic implications and the colonization of the Socotran archipelago. *Plant Systematics and Evolution* 265: 71–86.

THIV, M., M. THULIN, M. HJERTSON, M. KROPF, AND H. P. LINDER. 2010. Evidence for a vicariant origin of Macaronesian–Eritreo/Arabian disjunctions in *Campylanthus* Roth (Plantaginaceae). *Molecular Phylogenetics and Evolution* 54: 607–616.

THIV, M., M. THULIN, N. KILIAN, AND H. P. LINDER. 2006. Eritreo-Arabian affinities of the Socotran flora as revealed from the molecular phylogeny of *Aerva* (Amaranthaceae). *Systematic Botany* 31: 560–570.

THOMPSON, J. D., T. J. GIBSON, F. PLEWNIAK, F. JEANMOUGIN, AND D. G. HIGGINS. 1997. The ClustalX windows interface: Flexible strategies for multiple sequence alignment aided by quality analysis tools. *Nucleic Acids Research* 25: 4876–4882.

THORNE, J. L., AND H. KISHINO. 2002. Divergence time and evolutionary rate estimation with multilocus data. *Systematic Biology* 51: 689–702.

THORNE, J. L., H. KISHINO, AND I. S. PAINTER. 1998. Estimating the rate of evolution of the rate of molecular evolution. *Molecular Biology and Evolution* 15: 1647–1657.

THULIN, M. 1999. *Thamnosma* (Rutaceae) in Africa. *Nordic Journal of Botany* 19: 5–11.

THULIN, M., AND M. LAVIN. 2001. Phylogeny and biogeography of the *Ormocarpum* group (Fabaceae): A new genus *Zygocarpum* from the Horn of Africa region. *Systematic Botany* 26: 299–317.

TIFFNEY, B. H. 1980. Fruits and seeds of the Brandon Lignite, V. Rutaceae. *Journal of the Arnold Arboretum* 61: 1–40.

TIFFNEY, B. H. 1985a. Perspectives on the origin of the Floristic similarity between eastern Asia and eastern North America. *Journal of the Arnold Arboretum* 66: 73–94.

TIFFNEY, B. H. 1985b. The Eocene North Atlantic land bridge and its importance in Tertiary and modern phytogeography of the Northern Hemisphere. *Journal of the Arnold Arboretum* 66: 243–273.

VAN DAMME, K. 2009. Socotra archipelago. *In* R. G. Gillespie and D. A. Clague [eds.], Encyclopedia of islands, 846–851. University of California Press, Berkeley, California, USA.

VERDCOURT, B. 1969. The arid corridor between the northeast and southwest areas of Africa. *Palaeoecology of Africa* 4: 140–144.

VON BALTHAZAR, M., P. K. ENDRESS, AND Y.-L. QIU. 2000. Molecular phylogenetics of Buxaceae based on nuclear ITS and plastid ndhF sequences. *International Journal of Plant Sciences* 161: 785–792.

WIENS, J. J. 1998. Combining data sets with different phylogenetic histories. *Systematic Biology* 47: 568–581.

WIENS, J. J. 2004. Speciation and ecology revisited: Phylogenetic niche conservatism and the origin of species. *Evolution; International Journal of Organic Evolution* 58: 193–197.

WIKSTRÖM, N., V. SAVOLAINEN, AND M. W. CHASE. 2001. Evolution of angiosperms: Calibrating the family tree. *Proceedings of the Royal Society of London, B, Biological Sciences* 268: 2211–2220.

WOLFE, J. A. 1975. Some aspects of plant geography of the northern hemisphere during the late Cretaceous and Tertiary. *Annals of the Missouri Botanical Garden* 62: 264–279.

YANG, Z. 1997. PAML: A program package for phylogenetic analysis by maximum likelihood. *Computer Applications in the Biosciences* 13: 555–556.

YU, Y., A. J. HARRIS, AND X. J. HE. 2010. S-DIVA (Statistical dispersal–vicariance analysis): A tool for inferring biogeographic histories. *Molecular Phylogenetics and Evolution* 56: 848–850.